CONF-781202--7

PREPRINT UCRL-80790

Lawrence Livermore Laboratory

A LASER-DOPPLER VELOCIMETER FOR MEASURING DROPLET VELOCITIES IN TWO-PHASES LIQUID-DOMINATED NOZZLE FLOWS

T. W. Alger
C. T. Crowe
W. H. Giedt

This paper was prepared submission to
Symposium on "Measurements in Polyphase Flows" ASME Winter Annual Meeting
San Francisco, California, December 10-15, 1978

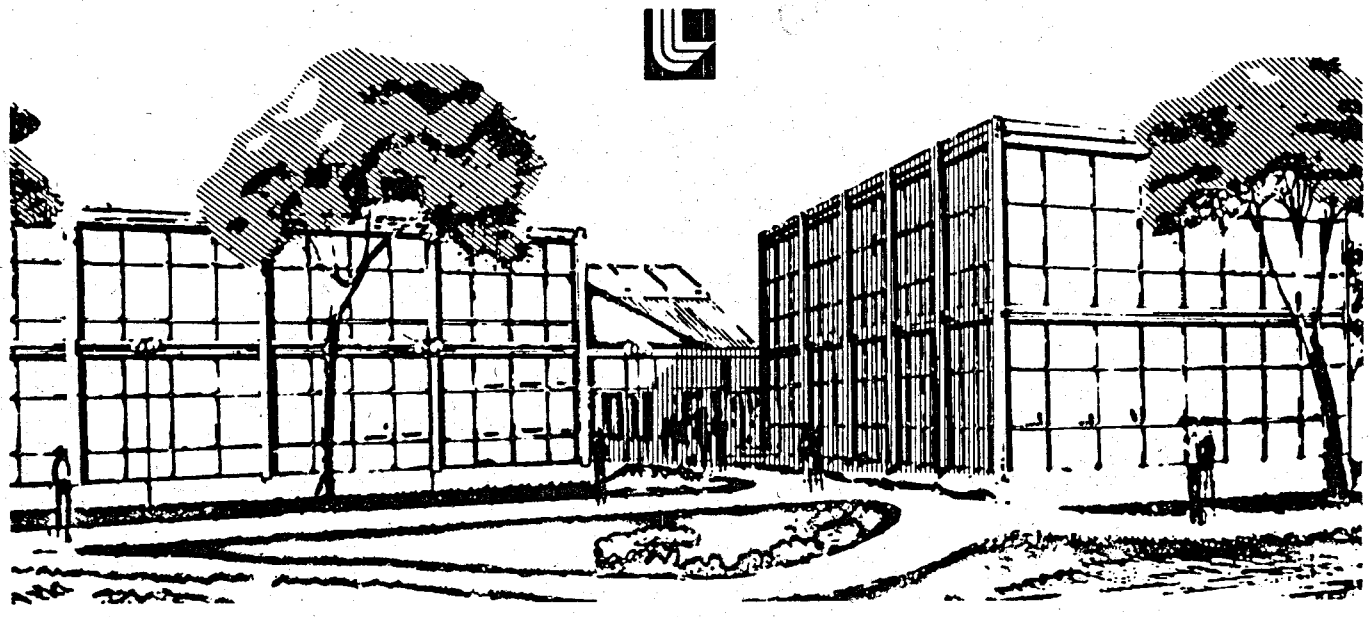

DISCLAIMER

A LASER-DOPPLER VELOCIMETER FOR MEASURING DROPLET VELOCITIES IN TWO-PHASE, LIQUID-DOMINATED NOZZLE FLOWS

T. W. Alger, C. T. Crowe, W. H. Gfedt

Lawrence Livermore Laboratory, University of California
Livermore, California 94550

ABSTRACT

A new laser-Doppler velocimeter (LDV) arrangement for measuring droplet velocities in high velocity, liquid-dominated two-phase nozzle flows was developed. The transmitting optics arrangement for this LDV system is identical to that of a dual beam heterodyne LDV, i. e., the light beam from a single frequency argon laser is divided into two parallel identical beams, which are focused to an intersection volume in the flow. The light backscattered from droplets traveling through this volume is collected for analysis using a scanning confocal Fabry-Perot interferometer (FPI). Because of the dual beam arrangement an unscattered or reference beam is not necessary, and the optical alignment ease and stability are greatly improved over similar LDV-FPI systems. Results of droplet velocity measurements in high velocity, high droplet concentration nozzle jet flows are presented.

NOMENCLATURE

c	- speed of light
d_{mv}	- LDV measurement volume diameter
D_b	- laser beam diameter
f	- frequency
F	- FPI finesse
F_l	- lens focal length
h	- enthalpy per unit mass
$\vec{k}_i$, $\vec{k}_s$	- LDV incident and scattered light direction unit vectors
l_{mv}	- LDV measurement volume length
P	- saturation pressure
r	- FPI mirror radius
R_D	- detected pulse rate from pulse generator
t_1, t_2	- oscilloscope trace times (distances)
T_{FSR}	- free spectral range (FSR) sweep period
u_d	- droplet velocity
$\vec{u}_d$	- droplet velocity vector
β	- LDV alignment angle
Δf	- Doppler frequency shift
Δf_{FSR}	- FPI frequency free spectral range
Δf_1, Δf_2	- Doppler frequency shift in light scattered from each beam of the dual beam backscatter LDV-FPI system
$\Delta\varphi$	- LDV collection aperture included angle
λ	- light wavelength
τ_R	- pulse integrator response time
φ	- LDV beam intersection half angle

Subscripts

d	- droplet phase
e	- nozzle exit
FSR	- free spectral range
i	- incident
o	- stagnation
s	- scattered

INTRODUCTION

One of the methods currently being investigated for the conversion of energy contained in extensively known liquid-dominated geothermal energy sources is based on the direct expansion of the available two-phase fluid mixture at the wellhead through an energy conversion device (1)-(3). This approach, which is known as the *total flow* process, would utilize the energy contained in both the liquid and vapor phases, and consequently, it would yield a greater energy conversion efficiency than the flashed steam systems currently in use.

One possible total flow device, which provided the impetus for this study, is an impulse turbine driven by a high velocity, two-phase mixture exhausting from a series of converging-diverging nozzles. Because of the high vapor volume fraction, the high fluid velocity and the negligible pressure gradient, the two-phase mixture in the nozzle jet can be considered to consist of small spherical droplets suspended in a vapor continuum. The efficient conversion of the energy in this high velocity, two-phase fluid by an impulse turbine requires small droplets (3), (4). The reason for this is that large droplets (> 4 μm based upon the theoretical predictions of reference (4)) will not follow the vapor streamlines within the turbine blade passages and will collide with the blade walls. This results in reduced momentum exchange and liquid film pumping losses.

A nozzle design which efficiently produces droplets with diameters < 4 μm is therefore essential for a maximum efficiency two-phase impulse turbine. Hence, it was determined that an experimental program to measure the droplet phase characteristics in liquid-dominated, two-phase nozzle flows was needed. The primary objective was to develop methods that would yield information concerning the droplet phase flow characteristics that are pertinent to both the impulse turbine blading and nozzle flow efficiences (i. e., droplet size distribution, droplet spatial distribution and droplet velocity) for two-phase,

steam-water mixtures characteristic of self-pumping geothermal wells.

Measurement of the droplet phase characteristics in single-component, two-phase, liquid-dominated nozzle flows is difficult because of the high velocities, the small droplet diameters, the high droplet number densities and the complex interphase transfer mechanisms. Conventional diagnostics, such as probing techniques, become unacceptable because of the serious perturbations introduced into the flow, or due to the harsh environment of the flow itself. For these reasons, passive measurement techniques based upon the scattering of light were developed. This report describes the considerations and experiments leading to the development of and experimental droplet velocity measurements with a particular laser-Doppler velocimeter (LDV) arrangement (droplet size and spatial distribution measurements are described in references (5) and (6)).

DOPPLER FREQUENCY SHIFT DETERMINATION

Measurement of the velocity of a moving droplet using a laser-Doppler velocimeter depends upon two basic physical principles. The first principle is that the droplet will scatter a fraction of any incident light. The second basic principle is that the light scattered from the moving droplet can be different in frequency from the incident light frequency. This frequency difference is proportional to the droplet velocity relative to the light source velocity and is commonly called the Doppler frequency shift. The Doppler frequency shift in the light scattered from a moving droplet for the geometry of Figure 1 is given by (7)

$$\Delta f = f_i - f_s = \left(\frac{\vec{u}_d}{\lambda_i}\right)\cdot(\vec{k}_i - \vec{k}_s) \qquad (1)$$

where the approximation that $c >> |\vec{u}_d|$ has been applied. Note that the index of refraction of the continuous phase has been assumed equal to 1.0.

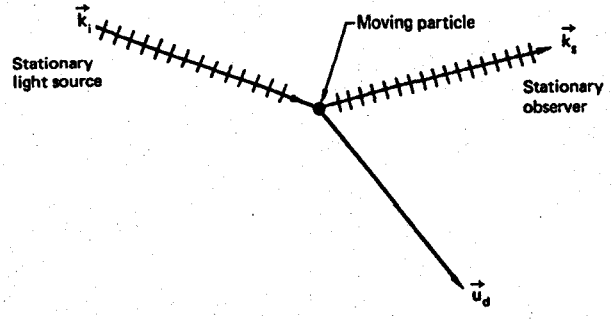

Figure 1. Diagram indicating the incident, $\vec{k}_i$, and scattered, $\vec{k}_s$, light direction unit vectors for a droplet moving with a constant velocity vector, $\vec{u}_d$.

The Doppler frequency shift given by equation (1) for a particle traveling at a speed corresponding to most physical continuum flow situations is very small when compared to the initial light frequency. One method for determining this small relative Doppler frequency shift is optical mixing spectroscopy. In optical mixing spectroscopy the scattered light beam is optically mixed with the incident light beam and passed into a square law photodetector (7), (8). The output of the square law detector is a beat frequency which is equal to the sum and difference of the incoming signal frequencies (the high frequency component is discarded due to photodetector response or electronic filtering). Thus, the measurement of the Doppler frequency difference is obtained directly, which eliminates the need for an absolute frequency measurement. LDV arrangements employing this method of Doppler frequency shift detection are commonly termed as heterodyne techniques, after the super-heterodyne techniques employed in radio frequency and microwave communications. Typically, the maximum Doppler frequency shift that can be determined in a heterodyne arrangement is near 100 MHz. This upper frequency limit is controlled by the photodetector and signal analysis electronics portion of the system.

A second method commonly employed for the Doppler frequency shift detection involves an optical instrument that allows an accurate determination of the wavelength of a beam of light. This instrument is known as the spherical mirror Fabry-Perot interferometer (FPI) (9). LDV systems generally incorporate the use of a scanning FPI for a relative, rather than absolute, determination of the Doppler frequency shift, i. e., the frequency (or wavelength) difference between the frequency shifted scattered light and a known light frequency standard is measured. This provides a direct optical measurement of the Doppler frequency difference.

In a typical LDV-FPI application, the optical arrangement is that of the reference beam mode in which both the scattered and unscattered light beams are mixed for frequency analysis using a confocal scanning FPI (see references (10) - (14)). However, several authors (e. g., (15) - (19)) have found that the single beam LDV arrangement also works well when using a Fabry-Perot interferometer for the Doppler frequency shift analysis.

The Doppler frequency shift in the scattered light is determined using a confocal FPI by piezoelectrically changing the distance between the mirrors. As this occurs, a changing interference pattern can be observed at the output of the FPI. The central interference fringe will become alternately bright and dark, depending upon whether the distance between the mirrors corresponds to an integral number of wavelengths (maximum intensity) or a half integral number of wavelengths (minimum intensity). For reference beam LDV-FPI operation, there will be bright fringes corresponding to the wavelengths (frequencies) of both the scattered and unscattered light beams. These bright fringes will occur at different spacings between the mirrors. The output of a photodetector monitoring these bright fringes is displayed on an oscilloscope as a function of the distance between the FPI mirrors. The Doppler frequency shift is proportional to the ratio of the distance between the scattered and reference beam signal peaks and the distance between consecutive reference beam peaks.

APPLICATION OF LDV FOR MEASUREMENTS IN HIGH VELOCITY, LIQUID-DOMINATED NOZZLE FLOWS

General Nozzle Design Operating Conditions

Nozzle operating conditions selected for testing are listed in Table 1 and were based on representative geothermal wellhead fluid states in the Salton Sea area of California (1). The nozzle exit pressure was based upon the minimum sink temperature available at the Salton Sea area on a warm summer day, thus providing a maximum nozzle exhaust velocity for efficient use of the geothermal energy resource.

Table 1. - Initial nozzle design operating conditions.

Variable	Inlet	Exhaust
Pressure	2.48 MPa (360 psia)	12.4 kPa (1.8 psia)
Temperature	224 C (435 F)	50 C (122 F)
Enthalpy	1.31 MJ/kg (563 Btu/lbm)	1.03 MJ/kg (444 Btu/lbm)
Vapor volume fraction	0.94	0.99984
Vapor mass fraction	0.189	0.346
Isentropic homogeneous exhaust velocity	———	742 m/s (2436 ft/s)
Droplet number per unit volume assuming a mean diameter of:		
10 μm	———	3.06 x 10^5/cm^3
5 μm	———	2.45 X 10^6/cm^3
1 μm	———	3.06 X 10^8/cm^3
Droplet separation in diameters	———	14.8

Table 1 presents several additional aspects of the two-phase fluid expansion. It can be seen that the vapor volume fraction is large throughout the nozzle flow, but the vapor mass fraction is small. This is interesting because it is the vapor phase that provides the compressibility effects necessary for the acceleration and breakup of the liquid phase. The small liquid phase volume fraction, when coupled with the high fluid velocity, allows the characterization of the two-phase fluid at the nozzle exit as a cloud of small spherical droplets dispersed throughout a vapor phase continuum. However, a consequence of the large relative amount of mass present in the liquid phase is a large number of droplets per unit volume dispersed throughout the nozzle flow. This factor is of major importance to the LDV measurements because of the light attenuation and scattering (for both incident and scattered light) and the measurement noise that can be caused by the high droplet number densities.

Doppler Frequency Shift and Measurement Volume Size

Measurement of the mean droplet velocity in high velocity, high droplet concentration nozzle flows using LDV techniques requires consideration of the maximum Doppler frequency shift, the measuring volume size, the laser power requirements and the configuration and alignment of the optical components. The maximum Doppler frequency shift and the measuring volume size are directly related to the beam intersection angle. Application of equation (1), to the common LDV arrangements shown in Figure 2, leads to the following relation for the Doppler frequency shift in terms of the beam intersection half angle, φ, the particle velocity, u_d, and the light wavelength, λ, (7), (8):

$$\Delta f = \frac{2\, u_d \sin \varphi}{\lambda} \qquad (2)$$

From this result, the Doppler frequency shift is seen to increase with an increase in the droplet velocity or an increase in the beam intersection angle for a given light wavelength. For high velocity flows, this frequency can easily be greater than the 100 MHz limit of the photodetector and electronics signal analysis equipment for a heterodyne LDV arrangement. This problem can be resolved by either reducing the beam intersection angle (e. g., at a droplet velocity of 1000 m/sec and a wavelength of 514.5 nm a beam intersection half angle of $\leq$ 1.5 degrees is required for the $\leq$ 100 MHz frequency limit), or a scanning confocal Fabry-Perot interferometer can be used for the resulting high frequency shift measurement.

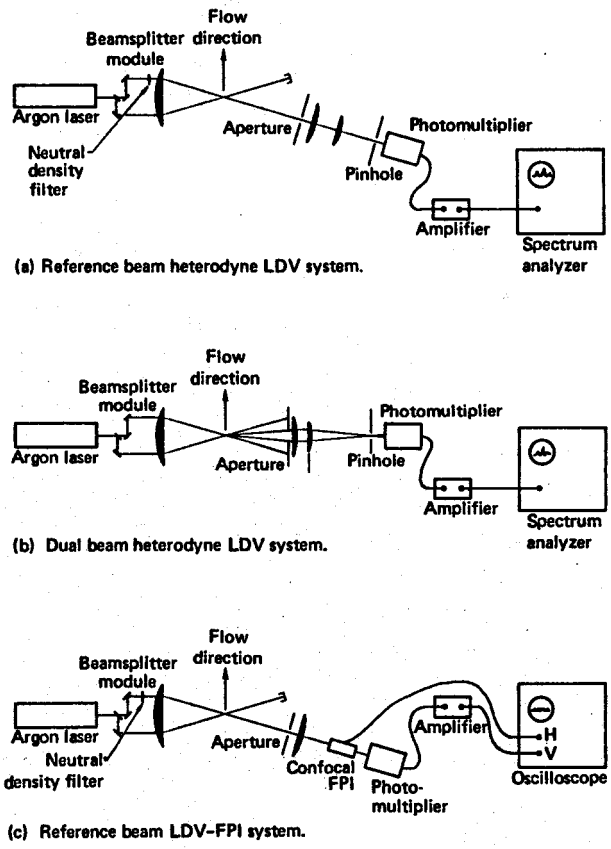

Figure 2. Schematic representations of three common LDV optical and signal analysis arrangements.

Doppler frequency shift reduction for high velocity flows by a reduction of the beam intersection angle results in an increase in the measuring volume. The effective diameter of the beam intersection region is given as (8)

$$d_{mv} = \frac{5\lambda F_t}{\pi D_b \cos \varphi} \qquad (3)$$

Here F_t is the transmitting lens focal length, and D_b is the initial laser beam diameter where the intensity has dropped to $1/e^2$ times the center intensity. The length of the measuring volume is given as (8)

$$l_{mv} = \frac{5\lambda F_t}{\pi D_b \sin \varphi} \qquad (4)$$

Thus, for a 1.5 degree beam intersection angle, an initial beam diameter of 0.25 cm, a light wavelength of 514.5 nm and a lens focal length of 40 cm, the measuring volume effective diameter is 0.13 mm and its effective length is 5.01 mm.

The use of a measuring volume of this length in a high velocity, high particle concentration nozzle flow can result in several difficulties. The length of the measuring volume could span a significant portion of the nozzle jet, resulting in no spatial resolution and the inclusion of velocity gradients due to the jet velocity profile within the measuring volume. Also, because of the high droplet concentration, there could be as many as 2600 droplets in the measuring volume (for 2 μm diameter droplets and the nozzle exhaust conditions of Table 1), which could result in frequency analysis problems. The combination of these effects severely limits the usefulness of the heterodyne LDV techniques for the high velocity, high droplet concentration nozzle flows. However, very small measuring volumes (resulting with very high Doppler frequency shifts) can be used with LDV-FPI systems operating in high velocity flows, which results in substantially improved spatial resolution and a significantly reduced number of droplets in the measuring volume. Because of these considerations, the LDV-FPI system became very attractive for use in this study.

Qualitative LDV Arrangement Comparisons for High Droplet Concentration Flows

To determine which LDV signal analysis technique, either the heterodyne method using a spectrum analyzer for frequency analysis or the direct optical method using a scanning confocal FPI, would be best suited for the high velocity, high droplet number density nozzle jet flow measurements, a series of comparative experiments were performed. A small converging-diverging nozzle (0.318 cm thick rectangular nozzle exit) operating with an air-water, two-phase mixture that approximated the high droplet number density of the steam-water nozzle jet flow was used. The droplet velocity at the nozzle exit was measured to be near 300 m/s, which proved to be sufficient to allow a comparison between the different LDV signal analysis techniques.

Three different LDV arrangements were compared: 1) the reference beam heterodyne (Figure 2(a)), 2) the dual beam heterodyne (Figure 2(b)) and 3) the reference beam scanning confocal FPI (Figure 2(c)). All the methods were operated in the forward scattering mode using a single frequency argon laser (λ = 514.5 nm).

Important results determined from these experimental comparisons were:

(1) At comparatively low droplet concentrations (light transmission > 70%), both the heterodyne arrangements required much less laser power (10 - 20 mW) than did the LDV-FPI arrangement (50 - 75 mW) for similar signal qualities.

(2) At moderate droplet concentrations (light transmission between 30% and 70%), the reference beam heterodyne system had a slightly better signal quality than did the dual beam heterodyne arrangement. However, the LDV-FPI system output signal quality was far superior to either of the heterodyne techniques.

(3) At high droplet concentrations (light transmission < 30%), the Doppler frequency shift for both heterodyne techniques was completely obscured by noise. This noise was presumably caused by both the large velocity gradients and the large number of droplets within the measuring volume. This condition was virtually unaffected by changes in laser power. At this nozzle flow condition, the output signal of the LDV-FPI arrangement showed an increased signal broadening (probably due to a wider droplet size spectrum and greater kinetic nonequilibrium effects). It was also more intense than those recorded previously. This indicated that there was more light available in the central bright fringe, probably due to the larger number of droplets scattering light to the interferometer.

Because of the favorable results obtained with the LDV-FPI arrangement for this series of qualitative experiments, a laser-Doppler velocimeter arrangement employing a scanning confocal Fabry-Perot interferometer was chosen to be used for the low-quality, steam-water nozzle jet flow droplet velocity measurements.

EXPERIMENTAL DUAL BEAM BACKSCATTER LDV-FPI SYSTEM

Experimental LDV System Optical Arrangement

Following the selection of the LDV-FPI arrangement as the system to be used, it was determined that the forward scattering reference beam operational mode was too cumbersome for practical use at the nozzle test station. The unit for measuring forward scattered light required a critical optical alignment on each side of the nozzle exhaust chamber. This was difficult to achieve and maintain because of both the inaccessibility and the large environmental temperature excursions (10 C (50 F) to 100 C (212 F) environmental temperature range).

Because of these problems, a dual beam backscatter LDV optical arrangement using a scanning confocal FPI for signal analysis was developed. This optical arrangement, shown schematically in Figure 3, uses a transmitting optics arrangement identical to that of a dual beam heterodyne LDV system. The light beam from a single frequency argon laser is divided into two parallel identical beams, which are focused to an intersection point (measuring volume) in the flow. The light backscattered from droplets traveling through this intersection region is collected by the receiving lens and corrected for spherical aberrations by a second lens to collimate the light scattered from

the measuring volume. This scattered light beam is then reduced in diameter and can be spatially filtered before analysis for the Doppler frequency shift using the confocal scanning FPI. The spatial filter pinhole in the backscattered light beam path can be used to insure that only radiation from the measuring volume is received. However, the spatial filter was not used for this work because it was found that through the proper adjustment of the spacing between the two lenses used for reducing the beam, the light scattered from flow locations other than the measuring volume could be caused to diverge, and an aperture located prior to the FPI entrance could be used to eliminate all but the nearly collimated light originating at the beam intersection region in the flow. This provided an optical arrangement that was very simple to align. The initial dual beam separation was 5.0 cm and the transmitting lens focal length was nominally 12.0 cm. This resulted in a beam crossing half angle of 12.65 degrees (this angle was accurately determined, and because of lens spherical aberrations it was different from that expected).

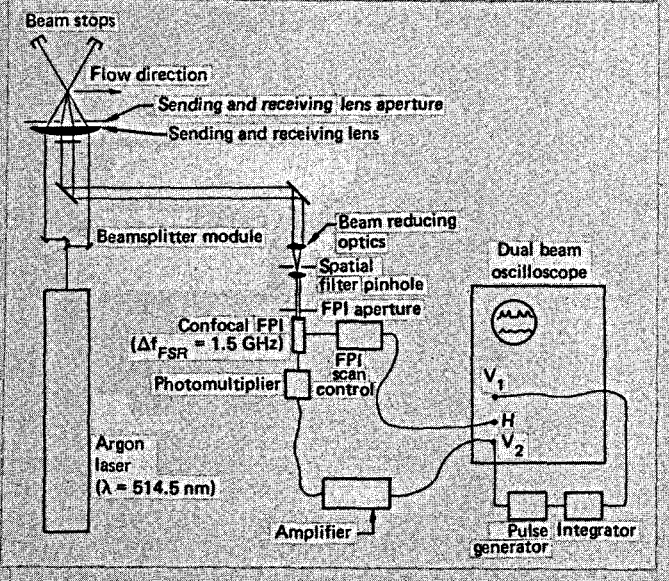

Figure 3. Dual beam backscatter LDV-FPI optical and signal analysis arrangements.

The dual beam backscatter LDV-FPI optical arrangement developed is unique in that a reference beam is not necessary to determine the Doppler frequency shift. This is because the dual beam LDV-FPI system utilizes light that has been scattered from two different focused laser beams at different angles with respect to the flow direction. The light scattered from one beam will have a higher frequency than that of the unscattered light, while the light scattered from the second beam will be lower in frequency. The difference in the frequency shifts between the two beams, when combined with the FSR characteristics of the FPI, provides all the information necessary for the Doppler frequency shift determination. The ease of alignment and the stability of this optical arrangement are greatly improved over those of other LDV-FPI optical arrangements because modular units can be readily utilized. Figure 4 is a photograph of the dual beam backscatter LDV-FPI unit showing the modular assembly.

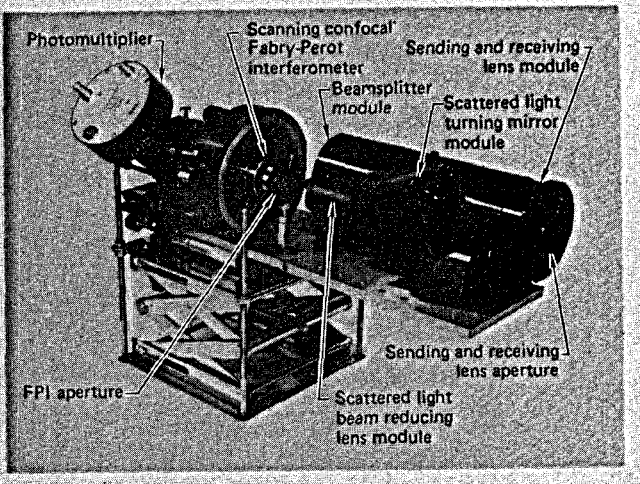

Figure 4. Photograph of the dual beam backscatter LDV-FPI modular assembly.

Doppler Frequency Shift Analysis

The Doppler frequency shift of the light scattered from a particle moving through the laser beam intersection region can be analyzed for the dual beam backscatter LDV-FPI system using the beam intersection geometry shown in Figure 5. From equation (1), the Doppler frequency shift of the light scattered from laser beam number 1 (incident from the forward direction) can be expressed in terms of the beam intersection and scattering geometry as

$$\Delta f_1 = \frac{u_d}{\lambda}\left[-\sin\beta\cos\varphi - \cos\beta\sin\varphi + \sin(\beta\pm\Delta\varphi)\right] \quad (5)$$

Similarly, the Doppler frequency shift associated with the light scattered from beam number 2 (incident from the rearward direction) becomes

$$\Delta f_2 = \frac{u_d}{\lambda}\left[-\sin\beta\cos\varphi + \cos\beta\sin\varphi + \sin(\beta\pm\Delta\varphi)\right] \quad (6)$$

Equations (5) and (6) each include a term that shows that the Doppler frequency shift in the light scattered from each beam is broadened by the physical size of the scattered light receiving aperture. This measurement error is called aperture broadening and is due to the finite included angle, $\Delta\varphi$, of the receiving lens aperture. It can be seen that large aperture sizes (large $\Delta\varphi$) can introduce significant errors into the measured frequency of the light scattered from either of the incident laser beams.

Defining the total Doppler frequency shift of the dual beam FPI system as the difference between the Doppler frequency shift of the scattered light from each of the two focused laser beams results in the equation

$$\Delta f = \Delta f_2 - \Delta f_1 = \frac{2u_d}{\lambda} \sin\varphi \cos\beta \qquad (7)$$

This equation reduces to that presented earlier (see equation (2)) when the optical system is aligned perpendicular to the droplet velocity vector ($\beta = 0$ degrees). This equation is an important result in that it indicates that the droplet velocity can be obtained using a dual beam LDV-FPI system without the complication of a reference beam signal. This fact greatly simplifies the backscatter optical arrangement, which enhances the optical alignment ease and stability. Also, equation (7) shows both that aperture broadening errors are nonexistant for this arrangement and that a reasonable amount of alignment error can be tolerated without significant measurement error (e. g., an error of < 1% is introduced for $\beta \leq 8$ degrees).

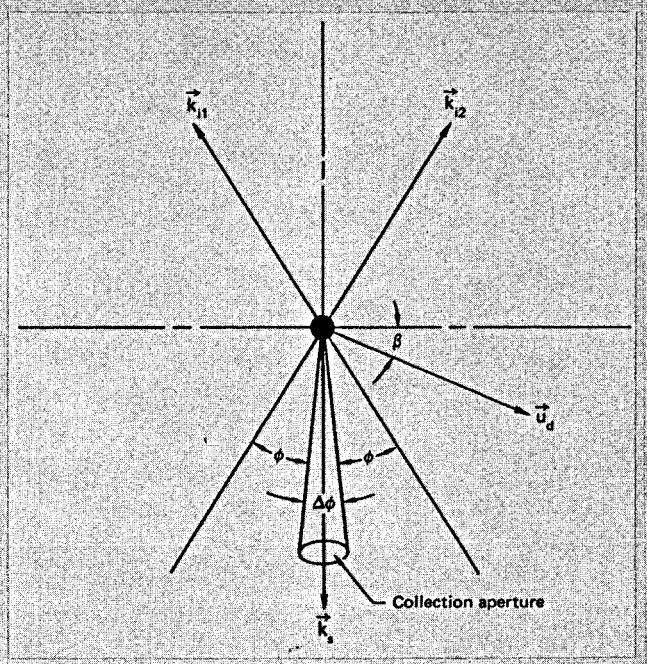

Figure 5. Light scattering geometry for the dual beam backscatter LDV-FPI optical arrangement.

Experimental Doppler Frequency Shift Determination

The electronic signal obtained using the LDV-FPI optical arrangement was analyzed using two different methods, each yielding different information. The electronic signal analysis equipment used for the backscatter LDV-FPI arrangement is shown schematically in Figure 3. The first method of signal analysis was to record the photomultiplier voltage output on an oscilloscope as a function of the distance between the FPI mirrors. A sawtooth voltage from the oscilloscope horizontal sweep was used to drive the piezoelectric crystals of the FPI. A typical result obtained using this signal analysis method is shown by the lower oscilloscope trace in Figure 6. Here the distance between the first (or second) set of peaks (indicated by t_2) is a measure of the Doppler frequency shift, Δf. The distance between the two sets of peaks (indicated by t_1) shown is a measure of the free spectral range (FSR) of the FPI. The FSR, Δf_{FSR}, of a confocal FPI is simply related to the radius of curvature of the mirrors, r, and the speed of light, c, according to (8)

$$\Delta f_{FSR} = \frac{c}{4r} \qquad (8)$$

Since t_1 in the oscilloscope trace is directly proportional to Δf_{FSR}, the Doppler frequency shift, which is proportional to t_2, can be simply calculated from

$$\Delta f = \left(\frac{t_2}{t_1}\right) \Delta f_{FSR} \qquad (9)$$

Introducing equation (9) into equation (7) yields the desired droplet velocity.

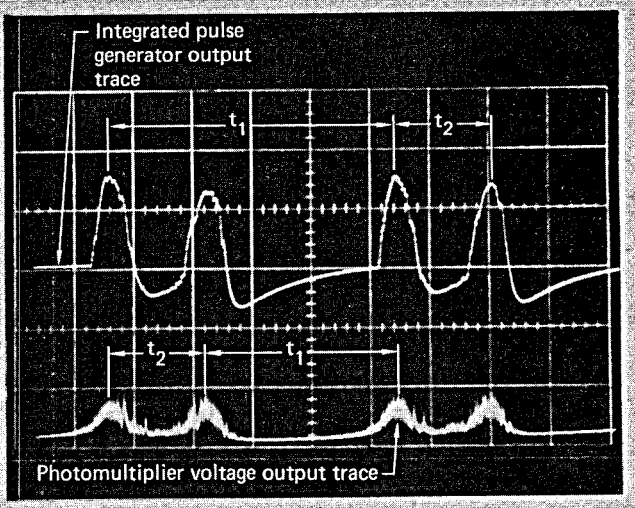

$$u_d = \left(\frac{t_2}{t_1}\right)\left(\frac{\Delta f_{FSR}\lambda}{2\sin\phi}\right) = 600 \text{ m/s}$$

Δf_{FSR} = 1.5 GHz
λ = 514.5 nm
ϕ = 12.65 degrees

Figure 6. Photograph of a typical oscilloscope trace for the dual beam backscatter LDV-FPI system.

The photomultiplier output trace shown in Figure 6 is actually an indication of the intensity of light scattered from droplets of varying sizes in the measurement volume. The horizontal spread or width of this curve is due to the fact that the droplets in the measurement volume have a velocity distribution. The local amplitude of the photomultiplier response curve exhibits variation because: 1) small droplets scatter less light than large droplets, and 2) there is a droplet size distribution in the measurement volume. The maximum scattered light intensity will result from a combination of droplet diameter and droplet number density. Although it is not possible to separate size

and number density effects, the peak of the photomultiplier output voltage will occur at a droplet size greater than the maximum of the droplet number density distribution.

The second method of LDV-FPI signal analysis used provided a display of the droplet number rate versus velocity. This was accomplished by converting each pulse from the photomultiplier, irrespective of its amplitude above a preset voltage, into a constant amplitude pulse using a pulse generator. This train of constant amplitude pulses from the pulse generator was then summed using an integrator prior to its display on an oscilloscope. A typical result obtained using this signal analysis method is shown by the upper oscilloscope trace in Figure 6. In this case, the distance between the first (or second) set of integrated pulse generator curve peaks (indicated by t_2) is a measure of the Doppler frequency shift, Δf. The distance between the two sets of peaks (indicated by t_1) shown is a measure of the free spectral range (FSR) of the FPI. Hence, the Doppler frequency shift and the droplet velocity can be calculated using equations (7) and (9), as presented previously.

With this type of signal monitoring, the local amplitude of the oscilloscope trace is proportional to the number of pulses received by the integrator for an essentially fixed spacing of the FPI mirrors. Hence, the number of pulses at any particular mirror separation distance is representative of the number of droplets having a certain velocity. The peak in the oscilloscope trace will therefore correspond to the velocity of the droplets for which the number density is a maximum. Again, the width of the integrated response curve is a measure of the droplet velocity distribution.

The combination of these two signal analysis techniques was used by Morse, et. al., (19), along with a numerical two-phase flow prediction method to determine particle size and velocity in two-phase rocket nozzle jet flows (see reference (20) for a similar concept for droplet size measurement using a heterodyne LDV method). As was described previously, the local photomultiplier signal amplitude trace is proportional to both the droplet size and the droplet number density. The integrated pulse generator output is proportional only to the droplet number density. Thus, from a comparison of the spatial location of the peaks in the two oscilloscope traces, a qualitative measure of the droplet size distribution function width can be obtained, i. e., the more horizontal separation between the peaks of the droplet number rate trace and and the photomultiplier voltage output trace, the greater the width (or multimodal nature) of the droplet size distribution function. These analyses cannot be combined to yield the droplet size directly, however, because of the many experimental unknowns that influence this measurement (see the discussion presented by Morse, et. al. (19) concerning this subject).

The pulse rate counter (integrator) functions by accumulating the output pulses of the pulse generator on a capacitor which is continually discharged by a resistor. In this manner, the capacitor voltage is a measure of the pulse rate averaged over the integration time. Denoting τ_R as the response or integration time and R_D as the rate of detected signal pulses, the output voltage is proportional to $R_D\tau_R$, which has a statistical fluctuation with a standard deviation of $(R_D\tau_R)^{1/2}$ (16). Since the relative standard deviation due to a finite count rate is proportional to $(R_D\tau_R)^{-1/2}$, τ_R should be made as large as possible. However, to avoid degradation in the velocity resolution the response time cannot exceed the time, T_{FSR}/F (T_{FSR} is the sweep period of the FPI and F is the finesse, i. e., a measure of the frequency resolving capability of the FPI). For the conditions of Table 1 and for 2 μm diameter droplets, the count rate is near 2.5×10^7 counts/s. The finesse of of the FPI used was near 100, and for a convenient FSR sweep rate of approximately 1 s, the integration time, τ_R, was set at 10 ms. These values yield a standard deviation in the count rate of 0.2%.

The FPI scan control unit of Figure 3 was constructed to provide better resolution of the Doppler frequency shift information. The oscilloscope sawtooth voltage was approximately 150 volts, but the FPI required only 40 volts per FSR scan. Thus, using the sawtooth voltage directly resulted with nearly four FSR scans per oscilloscope sweep. The scan control unit reduces the voltage at the FPI for better data resolution while maintaining time synchronization with the horizontal oscilloscope sweep. The use of this control regulates both the number of FSR's to be scanned per oscilloscope sweep and the oscilloscope sweep position at which the FPI FSR scan is to begin.

EXPERIMENTAL TWO-PHASE, STEAM-WATER NOZZLE AND TEST FACILITY

Two-Phase Test Facility and Nozzle Exhaust Chamber

The droplet phase characteristics studies were conducted using nozzles operating at the geothermal test facility at the Lawrence Livermore Laboratory (21). The test facility was designed to provide clean-water, two-phase flow conditions characteristic of those produced at the wellhead of self-pumping geothermal wells. Compressed liquid from a hot water generator is isenthalpically flashed to a two-phase mixture by a control valve prior to the nozzle entrance. The resulting two-phase mixture is then expanded through the test nozzle to an exhaust pressure controlled by a condenser - vacuum pump system combination. A flash control valve regulates the nozzle inlet pressure by controlling the total mass flow rate entering the nozzle. A liquid bypass line that connects the hot water generator directly with the condenser system is regulated by an automatic control valve to allow variations in nozzle mass flow rate (i. e., inlet pressure) to occur while maintaining the hot water temperature and pressure (i. e., enthalpy) constant.

Two-Phase Nozzle

The two-phase nozzle used for experimentation utilized a rectangular, converging-diverging cross-sectional geometry. The thickness of the nozzle parallel to the incident laser beam direction was constant at 0.325 cm. The nozzle throat height was 0.635 cm with a radius of curvature of 0.318 cm, and the nozzle exit to throat area ratio was 15.0. This thin nozzle geometry was chosen to provide the single scattering requirement necessary for the droplet size distribution and droplet spatial distribution measurements reported elsewhere (5), (6).

A photograph of the two-phase nozzle, as installed in the nozzle exhaust chamber, is shown in

Figure 7. This figure clearly indicates the complexity of the geometry required to contain the nozzle in a sealed vacuum chamber while maintaining the close coupling required by the optical arrangement. The diffuser was necessary to collect the nozzle jet flow to avoid window wetting and external (to the jet) scattering problems. However, window wetting did occur during warmup and when the nozzle was operating at off-design exhaust pressures, requiring the wiper arrangement for removing the spray prior to any measurements. Also, to avoid window condensation problems, it was found that the windows had to be maintained at a temperature higher than that of the fluid saturation state within the exhaust chamber. This condition was achieved by operating the exhaust chamber at atmospheric pressure (i. e., a temperature of 100 C (212 F)) to heat the windows prior to the droplet velocity measurements for which subatmospheric pressure was required.

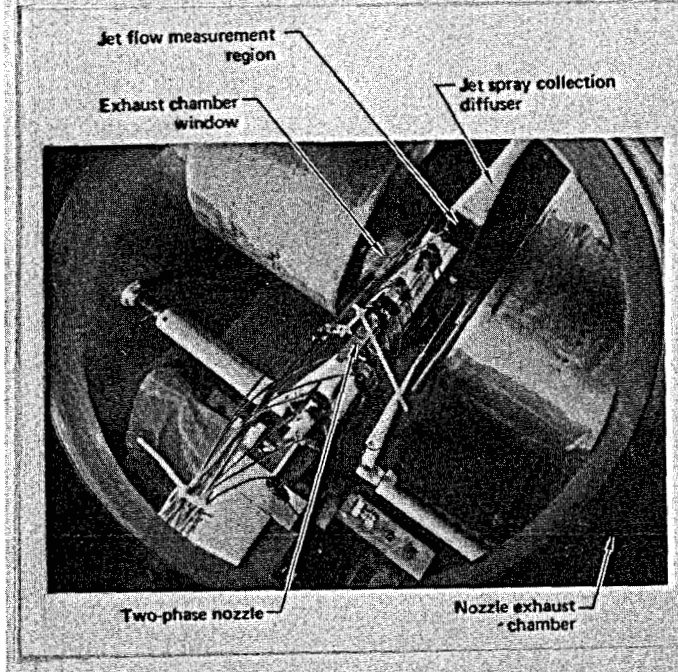

Figure 7. Top view photograph of the two-phase nozzle assembly installed in the nozzle exhaust chamber.

EXPERIMENTAL TWO-PHASE NOZZLE JET FLOW DROPLET VELOCITY MEASUREMENTS

During the initial experimental nozzle design, questions arose concerning the minimum nozzle thickness allowable to avoid serious boundary layer effects. A very thin nozzle jet flow was necessary to obtain the required light transmission for the light scattering experiments (5), (6). However, the conditions existing in large cross-section jet flows would yield information more representative of actual turbine nozzle operating conditions because of the smaller boundary layer and wall liquid film flow perturbations. To resolve this question concerning the nozzle operation and to demonstrate experimentally the spatial resolution of the dual beam LDV-FPI arrangement, droplet velocity profiles through the nozzle jet thickness were measured at the jet height centerline 1.0 cm from the nozzle exit, and at two different nozzle operating conditions. These velocity profiles are shown in Figure 8. The nozzle operating conditions at which these data were taken are listed in the figure. The velocities presented correspond to peak number density distribution droplet velocities, and thus, are the velocities corresponding to the greatest number of droplets in the flow. Droplet velocities determined from the photomultiplier voltage output differs from the velocities shown in Figure 8 by about 5%, and were therefore not included. The small difference between these two velocities and the near coincidence of the peaks of both the photomultiplier voltage output and the integrated pulse generator output on the oscilloscope trace (see Figure 6) indicated that the droplet size distribution function was narrow.

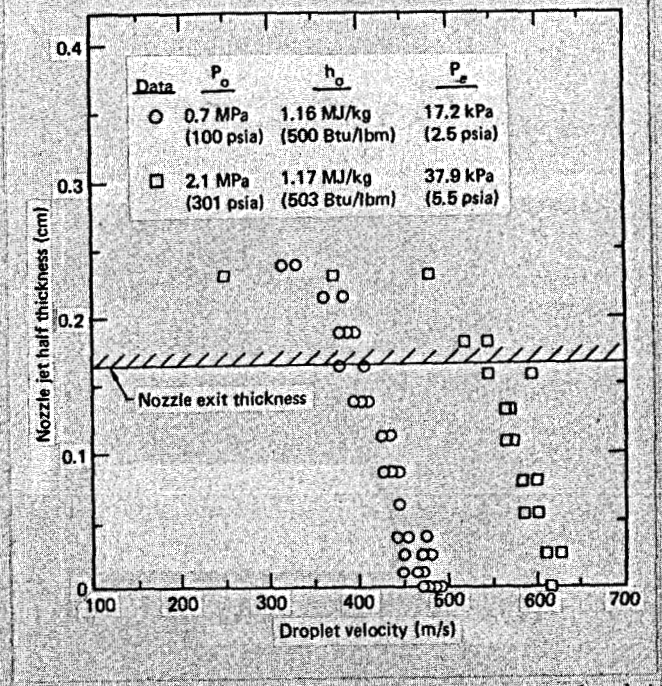

Figure 8. Peak number density distribution droplet velocity measurements across the jet flow half thickness.

A comparison of the velocity profiles of Figure 8 shows that there is little change in the basic profile due to the change in the inlet pressure. This indicates that the boundary layer effects are essentially the same in either case. A closer inspection of the two profiles shows a difference of approximately 100 m/s (328 ft/s) in the velocities of the two cases. However, a calculation based on isentropic, homogeneous flow indicates that the velocities corresponding to the different nozzle operating conditions should be nearly the same (approximately 600 m/s (1969 ft/s)). An analysis of the pressure profiles for the two cases shows that for the velocity profile corresponding to the 2.1 MPa

(300 psia) inlet pressure (exhaust pressure of 37.9 kPa (5.5 psia)) the nozzle was operating underexpanded, and for the velocity profile corresponding to the 0.7 MPa (100 psia) inlet pressure (exhaust pressure of 17.2 kPa (2.5 psia)) the nozzle was operating overexpanded. Overexpanded operation will cause an oblique shock to form in the nozzle jet flow. This could cause a velocity decrease before the fluid reached the measurement location 1.0 cm from the nozzle exit.

The maximum distance from the nozzle exit at which the oblique shocks would completely cross the jet flow (one shock originating at each sidewall) can be estimated. This estimation can be made because the velocity normal to an oblique shock wave must be greater than or equal to the local sonic velocity of the fluid. For a local two-phase sonic velocity of 230 m/s (755 ft/s) and a nozzle exhaust velocity of 600 m/s (1969 ft/s), the minimum angle that an oblique shock could form (at a sonic normal velocity) with respect to the nozzle axis is 22.5 degrees. Using this value indicates that the oblique shocks from each of the two nozzle sidewalls will intersect at a distance $\leq$ 0.4 cm from the nozzle exit (because of the 0.325 cm thick jet flow). Because this distance is less than the distance to the velocity measurement location (i. e., 1.0 cm from the nozzle exit) and because the two-phase oblique shock calculations of Comfort (4) indicate that the velocity loss for similar oblique shock conditions was approximately 100 m/s (328 ft/s), the difference in velocities between the two measured velocity profiles of Figure 8 appears to be caused by overexpanded nozzle operation for the 0.7 MPa (100 psia) inlet pressure conditions. Further measurements determined that for underexpanded nozzle operation at an inlet pressure of 0.7 MPa (100 psia), exhaust velocities near 600 m/s (1969 ft/s) were obtained. This velocity is very near that calculated for the vapor velocity using one-dimensional calculational methods (22), (23), and it subsequently indicated that small droplets were present in the nozzle jet flow (5). The large velocity difference between the two measured velocity profiles of Figure 8 suggests that underexpanded nozzle operation should be maintained to avoid oblique shock caused problems for free-stream velocity measurements in thin two-phase nozzle jet flows.

Although the velocity measurements of Figure 8 were made using a 0.325 cm jet thickness, the LDV-FPI system was found to allow measurements in much thicker nozzle jet flows. Velocity measurements in two-phase, air-water nozzle jet flows with light transmission characteristics similar to the steam-water nozzle flows have shown that the dual beam backscatter LDV-FPI arrangement was capable of measuring droplet velocities at depths up to 0.6 cm into the flow. This capability will allow free-stream velocity measurements to be obtained using large cross-section two-phase nozzles.

There were several possible sources of error involved in the droplet velocity measurements, with the largest error resulting from the peak to peak distance measurements from the oscilloscope traces. Inclusion of these errors indicates that droplet velocity measurement accuracies of better than ±3% at a 90% confidence level can routinely be expected. Both the accuracy and the data rate of this LDV-FPI system could be substantially improved by electronically determining the peak to peak distances (times) directly from the oscilloscope input voltages.

SUMMARY AND CONCLUSIONS

1) A new laser-Doppler velocimeter (LDV) utilizing a confocal Fabry-Perot interferometer (FPI) was developed to determine the droplet velocity in high velocity, high droplet concentration, two-phase nozzle jet flows. The basis of this system is a dual beam backscatter arrangement, for which the difference in frequency between the light scattered from each laser beam provides the Doppler frequency shift information. In this manner, a reference beam signal is not required, and the optical alignment ease and stability is enhanced over other LDV-FPI arrangements because modular optical assembly can be readily utilized.

2) The dual beam backscatter LDV-FPI arrangement was utilized to measure droplet velocity profiles in two-phase, steam-water nozzle jet flows. These measurements demonstrated the spatial resolution of the LDV-FPI arrangement, and they also indicated that the boundary layer effects for the thin cross-section nozzle flows (i. e. , 0.325 cm thick) were not sufficient to modify the maximum velocity at the nozzle exit. Maximum velocities near 600 m/s (1969 ft/s) were measured at the nozzle exit, corresponding very closely to the vapor exhaust velocity calculated using one-dimensional calculational methods.

3) Measurements in two-phase, air-water nozzle jet flows with similar light transmission characteristics as the steam-water nozzle flows demonstrated that velocity measurements could be obtained (using the dual beam backscatter LDV-FPI arrangement developed) at a depth up to 0.6 cm into the flow. This is sufficient to allow free-stream droplet velocity measurements in large cross-section nozzles.

ACKNOWLEDGEMENTS

The help and suggestions of Dr. F. Durst and Dr. S. A. Self during the initial portion of this work is greatfully acknowledged. Mr. D. L. Podesta was invaluable for the optical and nozzle equipment installations and modifications. Mr. C. W. Hall, Mr. D. W. Hansen, Mr. L. L. Jackson and Mr. G. H. Lathrop were of great assistance for the nozzle testing and maintenance. This work was performed under the auspices of the U. S. Department of Energy by the Lawrence Livermore Laboratory under contract number W-7405-Eng-48.

REFERENCES

1. Austin, A. L., Higgins, G. H., and Howard, J. H., "The Total Flow Concept for Recovery of Energy from Geothermal Hot Brine Deposits", UCRL-51366, Apr. 1973, Lawrence Livermore Laboratory, Livermore, California.

2. Austin, A. L. and Lundberg, A. W., "A Comparison of Methods for Electric Power Generation from Geothermal Hot Water Deposits", ASME Paper No. 74-WA/ENER-10, Nov. 1974.

3. Austin, A. L., "Prospects for Advances in Energy Conversion Technologies for Geothermal Energy Development", Proceedings of the Second United Nations Symposium on the Development and Use of Geothermal Resources, Vol. 3, May 1975, pp. 1925-1935.

4. Comfort, W. J., "The Design and Evaluation of a Two-Phase Turbine for Low-Quality Steam-Water Mixtures", D. Eng. Thesis, May 1977, University of California at Davis, Davis, California.

5. Alger, T. W., "Droplet Phase Characteristics in Liquid-Dominated Steam-Water Nozzle Flow", Ph. D. Thesis, Aug. 1978, University of California at Davis, Davis, California.

6. Alger, T. W. and Giedt, W. H., "A Light Scattering Technique for Determining Droplet Size Distributions in Two-Phase Liquid-Dominated Nozzle Jets", Proceedings of the First International Conference on Liquid Atomization and Spray Systems, Tokyo, Japan, Aug. 1978.

7. Watrasiewicz, B. M. and Rudd, M. J., Laser Doppler Measurements, Butterworths, London, 1976.

8. Durst, F., Melling, A., and Whitelaw, J. H., Principles and Practice of Laser-Doppler Anemometry, Academic Press, New York, 1976.

9. Hercher, M., "The Spherical Mirror Fabry-Perot Interferometer", Applied Optics, Vol. 7, No. 5, May 1968, pp. 951-966.

10. Jackson, D. A. and Paul,D. M., "Measurement of Hypersonic Velocities and Turbulence by Direct Spectral Analysis of Doppler Shifted Laser Light", Phys. Letters, Vol. 32A, No. 2, June 1970, pp. 77-78.

11. Jackson, D. A. and Paul, D. M., "Measurement of Supersonic Velocity and Turbulence by Laser Anemometry", Journ. Phys. E: Scientific Instruments, Vol. 4, Mar. 1971, pp. 173-177.

12. Paul, D. M. and Jackson, D. A., "Rapid Velocity Sensor Using a Static Confocal Fabry-Perot and a Single Frequency Argon Laser", Journ. Phys. E: Scientific Instruments, Vol. 4, Mar. 1971, pp. 170-172.

13. Eggins, P. L., Jackson, D. A., and Paul, D. M., "Measurement of Mean Velocity and Turbulence in Supersonic Boundary Layers, Shock Waves and Free Jets by Laser Anemometry", Opto-electronics, Vol. 5, No. 1, Jan. 1973, pp. 91-99.

14. Avidor, J. M., "Novel Instantaneous Laser Dopplet Velocimeter", Applied Optics, Vol. 13, No. 2, Feb. 1974, pp. 280-285.

15. James, R. N., Babcock, W. R., and Seifert, H. S.,"A Laser-Doppler Technique for the Measurement of Particle Velocity", AIAA Journ.,Vol. 6, No. 1, Jan. 1968, pp. 160-162.

16. Self, S. A., "Laser Doppler Anemometer for Boundary Layer Measurements in High Velocity, High Temperature MHD Channel Flows", Proceedings of the Second International Workshop on Laser Velocimetry, Vol. 2, Mar. 1974, pp. 44-67.

17. Daily, J. W., Kruger, C. H., Self, S. A., and Eustis, R. H., "Boundary-Layer Profile Measurements in a Combustion Driven MHD Generator", AIAA Journ., Vol. 14, No. 8, Aug. 1976, pp. 997-1005.

18. Self, S. A. and Kruger, C. H., "Diagnostic Methods in Combustion MHD Flows", Journ. of Energy, Vol. 1, No. 1, Jan. - Feb. 1977, pp. 25-43.

19. Morse, H. L., Tullis, B. J., Seifert, H. S., and Babcock, W., "Development of a Laser-Doppler Particle Sensor for the Measurement of Velocities in Rocket Exhausts", Journ. of Spacecraft and Rockets, Vol. 6, No. 3, Mar. 1969, pp. 264-272.

20. Yanta, W. J., "Measurements of Aerosol Size Distributions with a Laser Doppler Velocimeter (LDV)", AIAA Paper No. 73-705, July 1973.

21. Weiss, H. and Shaw, G., "Geothermal Two-Phase-Flow Test Facility", Proceedings of the Second United Nations Symposium on the Development and Use of Geothermal Resources, Vol. 3, May 1975, pp. 2065-2068.

22. Comfort, W. J., Alger, T. W., Giedt, W. H., and Crowe, C. T., "Calculation of Two-Phase Dispersed Droplet-in-Vapor Flows Including Normal Shock Waves", ASME Paper No. 76-WA/FE-31, Dec. 1976.

23. Crowe, C. T. and Comfort, W. J., "Atomization Mechanisms in Single-Component, Two-Phase, Nozzle Flows", Proceedings of the First International Conference on Liquid Atomization and Spray Systems, Tokyo, Japan, Aug. 1978.